CORA Cork Open Research Archive
Cartlann Taighde Oscailte Chorcaí

Title	Lead oxide-modified TiO2 photocatalyst: tuning light absorption and charge carrier separation by lead oxidation state
Authors	Iwaszuk, Anna;Nolan, Michael
Publication date	2013-05-09
Original Citation	Iwaszuk, A. and Nolan, M. (2013) 'Lead oxide-modified TiO2 photocatalyst: tuning light absorption and charge carrier separation by lead oxidation state', Catalysis Science & Technology, 3(8), pp. 2000-2008. http://dx.doi.org/10.1039/C3CY00194F
Type of publication	Article (peer-reviewed)
Link to publisher's version	10.1039/c3cy00194f
Rights	© The Royal Society of Chemistry 2013. This is the Accepted Manuscript version of a published work that appeared in final form in Catalysis Science & Technology, http://dx.doi.org/10.1039/C3CY00194F
Download date	2026-11-16 13:17:19
Item downloaded from	https://hdl.handle.net/10468/2923



UCC
University College Cork, Ireland
Coláiste na hOllscoile Corcaigh

Journal Name

Dynamic Article Links ►

Cite this: DOI: 10.1039/c0xx00000x

www.rsc.org/xxxxxx

ARTICLE TYPE

Lead Oxide-Modified TiO_2 Photocatalyst: Tuning Light Absorption and Charge Carrier Separation by Lead Oxidation State

Anna Iwaszuk and Michael Nolan

Received (in XXX, XXX) Xth XXXXXXXXX 20XX, Accepted Xth XXXXXXXXX 20XX

DOI: 10.1039/b000000x

Modification of TiO_2 with metal oxide nanoclusters such as FeO_x, NiO_x has been shown to be a promising approach to the design of new photocatalysts with visible light absorption and improved electron/ hole separation. To study further the factors that determine the photocatalytic properties of structures of this type, we present in this paper a first principles density functional theory (DFT) investigation of TiO_2 rutile (110) and anatase (001) modified with PbO and PbO_2 nanoclusters, with Pb^{2+} and Pb^{4+} oxidation states. This allows us to unravel the effect of the Pb oxidation state on the photocatalytic properties of PbOx-modified TiO_2, The nanoclusters adsorb strongly at all TiO_2 surfaces, creating new Pb-O and Ti-O interfacial bonds. Modification with PbO and PbO_2 nanoclusters introduces new states in the original band gap of rutile and anatase. However the oxidation state of Pb has a dramatic impact on the nature of the modifications of the band edges of TiO_2 and on the electron/hole separation mechanism. PbO nanocluster modification leads to an upwards shift of the valence band which reduces the band gap and upon photoexcitation results in hole localisation on the PbO nanocluster and electron localisation on the surface. By contrast, for PbO_2 nanocluster modification the hole will be localised on the TiO_2 surface and the electron on the nanocluster, thus giving rise to two different band gap reduction and electron-hole separation mechanisms. We find no crystal structure sensitivity, with both rutile and anatase surfaces showing similar properties upon modification with PbOx. In summary the photocatalytic properties of heterostructures of TiO_2 with oxide nanoclusters can be tuned by oxidation state of the modifying metal oxide, with the possibility of a reduced band gap causing visible light activation and a reduction in charge carrier recombination.

1. Introduction

TiO_2 plays an important role in photocatalysis due to its properties, including relatively low cost, availability and non-toxicity. These properties make TiO_2 suitable as a photocatalyst for water-splitting technology using renewable resource in the form of solar light,[1,2] or for depollution of toxic organic pollutants from the domestic and industry use.[3-5] However the band gap of TiO_2 which lies in the range of 3.0 to 3.2 eV (depending on the crystal form) can only absorb in the UV region. It is therefore important to find a means to reduce the band gap and make TiO_2 active in the visible region.[6] There are several ways to achieve this target and one of these is so-called "band gap engineering" which is focused on substitution of metal cations and/or non-metal anions at Ti and O sites in rutile or anatase.[7-14] There are many experimental[15-17] and theoretical[18] efforts in band gap engineering and while the results are promising, there are still important practical issues like stability, solubility and reproducibility that may limit TiO_2 doping for photocatalyst production. Another important aspect of photocatalyst efficiency is recombination of photoexcited electrons and holes (charge carriers) and we need to understand how modifying TiO_2 impacts this important factor.

Nanoscale heterostructures composed of two different structures interfaced together can be used to improve the photocatalytic properties of TiO_2 or any other oxide. Research in this field shows that the interface between two materials play an important role in tuning photocatalytic properties and inducing activity of material in the visible region.[18-24] Recent examples of such heterostructures are BiOBr-$ZnFe_2O_4$[25], AgI-BiO[26] and $BiVO_4$-WO_3[27], where improved activity in the visible region has been reported.

Fabrication of interesting heterostructures of TiO_2 modified with dispersed, molecular scale metal oxide nanoclusters has been presented by Libera[24] et al (using atomic layer deposition ALD) and Tada[28,29] et al (using chemisorption-calcination CCC) for FeOx-modified TiO_2. In both experiments, similar results in terms of band gap reduction and photocatalytic activity were found and the results are explained by the presence of FeO_x cluster derived electronic states lying at the valence band of TiO_2 and pushing the valence band edge up in energy. Moreover the results of photoluminescence spectroscopy revealed a reduction in electron/hole recombination explained by suppression of the PL TiO_2 peak at 540nm.[28] Using first principles density functional theory simulations of models of metal oxide

nanocluster modified TiO_2, we have previously shown that $(FeO)_x$,[29] $(NiO)_x$[30] and (SnO_2)[31] nanoclusters supported on TiO_2 can reduce the band gap and improve the photocatalytic properties of heterostructures. We have also found that oxide nanocluster modifications of TiO_2 may also result in no effect in terms of band gap reduction, for example, supported SnO_2 nanoclusters on anatase (001) have no impact on the anatase band gap.[31]

A comparison of SnO and SnO_2 modified TiO_2 in our DFT simulations[31,32] shows the dramatic effect of the metal oxidation state – with SnO modification reducing the anatase band gap and SnO_2 modification having no effect. An experiment from Boppana and Lobo[33] examined $ZnGa_2O_4$ modified with SnO and SnO_2 and these authors also found a dramatic effect arising from Sn oxidation state, with only SnO modified $ZnGa_2O_4$ showing visible light activity, but no detailed explanation for this effect was presented. We have suggested that the presence of the Sn(II) stereochemical lone pair in SnO is the origin of the difference between SnO and SnO_2 modified TiO_2[31,32]. Thus, it appears that there is great potential in examining how metal oxides with variable oxidation states and a stereochemical lone pair could be used to modify TiO_2 for visible light absorption.

Motivated by this idea, in this paper we present results for models of rutile (110) and anatase (001) modified with PbO and PbO_2 nanoclusters and investigate further how the oxidation state of the metal (Pb^{2+} vs. Pb^{4+}) impacts the energy gap of TiO_2 and how this idea may be useful for photocatalyst design based on surface modified metal oxides.

2. Computational Methods

To model TiO_2 rutile (110) and anatase (001) surfaces, we use a three dimensional periodic slab model within the VASP code.[34] The valence electrons are described by a plane wave basis set and the cut-off for the kinetic energy is 396 eV. The core-valence interaction is described by PAW potentials[35] and the number of valence electrons is 4 for Ti, 4 for Pb and 6 for O. The exchange-correlation functional was approximated by the Perdew-Wang 91[36] functional. We use a Monkhorst-Pack (2×1×1) k-point sampling grid.

To describe Ti 3d states the DFT+U approach was used where U=4.5 eV. The need to introduce the U parameter in order to describe properly d shells in transition metals is well known.[37-41]

For Pb, the electronic states for Pb^{2+} and Pb^{4+} oxidation states are consistently described by DFT so no U correction is applied. While the DFT+U approach gives a consistent description of the Ti 3*d* electronic states, it will still underestimate the band gap. This is of course an important issue, however, we are primarily concerned with qualitative changes in the band gap upon surface modification, that is whether the metal oxide nanocluster reduces the energy gap or not and for this, DFT+U is sufficiently useful.

The rutile (110) and anatase (001) surfaces are used as the initial substrates for modification with PbO_x nanoclusters. The rutile (110) surface is the most widely studied TiO_2 surface and the most likely to be used in any experimental work. This surface has two-fold coordinated bridging O atoms, 5-fold coordinated surface Ti atoms and 6-fold coordinated surface Ti atoms. A (2x4) surface supercell expansion is employed to allow isolated nanoclusters to be adsorbed. The anatase (001) surface, while not the most stable anatase surface, has been of great interest for its potential photocatalytic activity and is considered here for this reason. In our work, we study anatase (001) as an unreconstructed surface, which is reasonable to describe this surface. Some preliminary calculations of anatase (101) modified with lead oxide nanoclusters indicate no significant effects as a result of the surface used. The (001) surface is terminated by two-fold coordinated oxygen atoms while the oxygen atoms in the surface are three coordinated. The Ti atoms in the surface are 5-fold coordinated. A (4×2) surface supercell is used. Both surface models are stoichiometric with no defects and no adsorbed hydroxyl species, both of which are well known defects in TiO_2 surfaces and a 12 Å vacuum gap is used. The convergence criteria for the electronic and ionic relaxations are 0.0001 eV and 0.02 eV/ Å. For the consistency in the calculation, we also applied the same supercell and technical parameters for the bare TiO_2 surface and free clusters.

The clusters are positioned on the TiO_2 surfaces and the adsorption energy is computed from:

$$E\text{ads} = E((PbO_x)\text{-}TiO_2) - \{ E(PbO_x) + E(TiO_2) \} \quad (1)$$

Where $E((PbO_x)\text{-}TiO_2)$ is the total energy of the PbO_x (PbO or PbO_2) nanocluster supported on the anatase surface and E(PbO) and $E(TiO_2)$ are the total energies of the free PbO cluster and the unmodified anatase surface. A negative adsorption energy indicates that cluster adsorption is stable.

To study a model of the photoexcited electronic state of PbO-modified anatase and examine how the Pb oxidation state determines the electron and hole trapping, we take the $(PbO)_4$ and Pb_2O_4-modified rutile models as examples and generate a triplet electronic state,[42,43,44] in which we have an excited electron in the conduction band and a hole in the valence band. To describe reduced Ti^{3+} that are formed we continue to use DFT+U (U = 4.5 eV on the Ti 3*d* states). However, we also have to properly describe the localized hole formed after excitation and the DFT+U approach is also applied to the O 2*p* states,[32,45] with a Hubbard U of 5.5 eV sufficient to give valence band hole localisation.[32,44] The following calculations are performed:

a single point energy of the triplet at the singlet geometry, $E^{\text{unrelaxed}}$

a full ionic relaxation in the triplet electronic configuration, $E^{\text{relaxed.}}$

A dipole correction perpendicular to the surface plane is added to the total energies. Within this computational set-up, the following energies are calculated:

(1) The singlet-triplet vertical unrelaxed excitation energy: $E^{\text{vertical}} = E^{\text{singlet}} - E^{\text{unrelaxed}}$, where the singlet (ground state) is fully relaxed and the triplet is fixed at the ground state geometry. This should correspond to the simple VB-CB energy gap from the density of states.

(2) The singlet-triplet vertical excitation energy: $E^{\text{excite}} = E^{\text{singlet}} - E^{\text{relaxed}}$, where both the singlet and triplet electronic states are fully relaxed. The change in this energy with respect to the bare surface allows us to determine the effect of the surface modification on the energy gap of TiO_2.

(3) The triplet relaxation (or trapping) energy: $E^{\text{relax}} = E^{\text{relaxed}} - E^{\text{unrelaxed}}$, where the first energy is the fully

This journal is © The Royal Society of Chemistry [year]

relaxed triplet and the second energy is the triplet state at the singlet geometry (from (1) above), so that E^{relax} is the energy gained when the electron and hole are trapped at their Ti and O sites upon structural relaxation.

3. Results and Discussion

3.1 PbO and PbO_2 Nanoclusters Supported on TiO_2 Rutile (110)

Figure 1 presents the relaxed atomic structures together with adsorption energies for representative PbO_x nanoclusters supported on the model rutile (110) surface: PbO, Pb_2O_2, Pb_4O_4, and Pb_2O_4, Pb_3O_6, Pb_4O_8. All clusters adsorb strongly at the surface with adsorption energies in the range from -2.81 eV to -7.16 eV and creating new interfacial metal-oxygen bonds. The magnitude of the adsorption energies indicates that the adsorbed nanoclusters will be stable to aggregation.

Table 1 presents the details of the new metal-oxygen bonds between the clusters and the surface. The smallest cluster, PbO, supported on rutile (110) creates three new bonds: Pb surface metal bonds to O cluster atoms with two bonds (2.25 Å, 2.45 Å) and the third bond between O cluster atom and Ti surface atom is 1.80 Å. In bulk litharge structured PbO, the Pb-O distances are 2.35 Å[46] and in the free PbO clusters, the Pb-O distances are in the range of 1.97 – 2.22 Å, so that the increased Pb coordination in the supported clusters leads to longer Pb-O distances that are reasonable for the Pb^{2+} oxidation state.

The Pb_2O_2 cluster results in seven new bonds: there are five bonds between Pb atoms and O atoms with the distances from 2.26Å to 2.61Å. The next two bonds between O cluster atoms and Ti surface atoms have the distances 1.78Å and 1.92Å. The adsorption of the biggest Pb_4O_4 cluster results in five new bonds: three bonds between Pb cluster atoms and O surface atoms with distances 2.31Å, 2.45Å and 2.55Å and the next two bonds from O cluster atoms and Ti surface atoms have distances 1.89Å and 1.89Å.

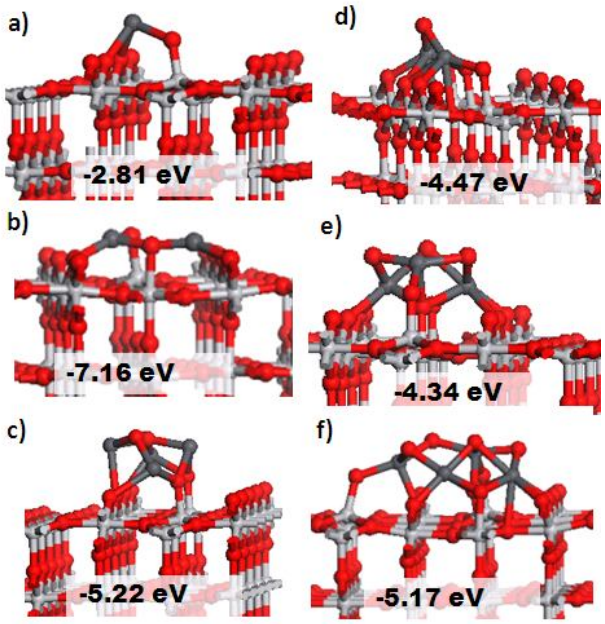


Fig. 1 Relaxed adsorption structures with adsorption energies given in eV for (a)PbO, (b)Pb_2O_2, (c)Pb_4O_4, (d)Pb_2O_4, (e)Pb_3O_6 and (f)Pb_4O_8 nanoclusters supported on TiO_2 rutile (110).

Pb_2O_4 and Pb_3O_6 clusters, with Pb^{4+} oxidation state, adsorbed on rutile (110) form seven new bonds: four bonds from Pb cluster atoms and O surface atoms with distances from 2.29 Å to 2.52 Å and three from O cluster atoms and Ti surface atoms with the lengths in the range 1.85 Å -1.99 Å. The biggest Pb_4O_8 cluster adsorbs on rutile surface creating nine new bonds: five between Pb cluster atoms and O surface atoms with distances from 2.15 Å to 2.65 Å and four other bonds from O cluster atoms and Ti surface atoms from 1.82 Å to 2.06 Å. The Pb-O distances in the PbO_2 nanoclusters are longer than in bulk rutile structured PbO_2, where they are 2.15 and 2.17 Å.

Table 1. New surface-cluster Pb-O bond distances for PbO and PbO_2 nanoclusters absorbed on TiO_2 rutile (110).

	Distances / Å				
	Pb_c-O_s [a]	O_c-Ti_s [b]		Pb_c-O_s [a]	O_c-Ti_s [b]
PbO	2.25; 2.45	1.80	Pb_2O_4	2.29; 2.52; 2.48; 2.29	1.96; 1.99; 1.96
Pb_2O_2	2.52; 2.60; 2.56; 2.61, 2.26	1.93; 1.78	Pb_3O_6	2.44; 2.30; 2.44; 2.30	1.91; 1.99; 1.85
Pb_4O_4	2.31; 2.45; 2.55	1.89; 1.88	Pb_4O_8	2.15; 2.23; 2.65; 2.39; 2.33	1.91; 2.02; 1.82; 2.06

[a] Pb from the cluster (Pb_c) and O from the surface (O_s) [b] O from the cluster (O_c) and Ti from the surface (Ti_s)

In all heterostructures Ti atoms in the (110) surface are pulled out of the surface when bonded to O atoms from the clusters: by 0.74Å for the PbO cluster and by 0.91Å for the biggest Pb_4O_8

cluster.

Figure 2 presents the electronic density of states projected (PEDOS) onto Pb *6s* and O 2*p* states of the supported PbO and PbO_2 nanoclusters and the Ti 3*d* and O *2p* states of the rutile (110) surface. The PEDOS plot is presented here in order to investigate the changes to the valence and conduction band edges due to adsorption of the lead oxide nanoclusters. In each case the zero of energy is the top of the occupied states. Considering firstly the PbO nanoclusters, the smallest PbO nanocluster does not introduce new states into the band gap of TiO_2 when adsorbed at the rutile (110) surface. The $(PbO)_2$ nanocluster results in the presence of cluster derived Pb and O states at the top of the VB. The biggest $(PbO)_4$ nanocluster introduces new PbO derived electronic states above the VB edge of TiO_2, which gives a significant reduction in the energy gap of TiO_2 while at the same time leaving the conduction band unchanged, so that the energy gap between the TiO_2 surface VB and CB is unchanged over unmodified TiO_2.

These new electronic states derived from the nanocluster will result in a narrowing compared to the original energy gap of TiO_2 because the valence band edge now lies higher in energy. The PEDOS plot for Pb_4O_4 supported on TiO_2 gives an indicative VB shift of 1eV compared to original TiO_2 band gap, which would result in visible light absorption. We note however that these energy differences are simply Kohn Sham eigenvalue differences and in a later section will examine this in more detail.

Contrary to this, the results for PbO_2 supported nanoclusters show no change in the region of the valence band of TiO_2 while new electronic states derived from empty Pb 6s states lie in the energy gap, below the conduction band edge of TiO_2. These new states can function as states into which an electron from the (unmodified) TiO_2 valence band can be excited, thus giving an effectively reduced energy gap when compared to unmodified TiO_2 (again the surface VB-CB energy gap is unchanged upon modification). In this case, the energy gap underestimation with DFT is clearly apparent, as in the largest Pb_4O_8 nanocluster, the empty Pb states are found *ca.* 0.9 eV above the VB edge. However, the important point is that the modification of TiO_2 with PbO_2 does lead to a reduction in the energy gap.

The nature of the VB and CB in the different PbOx modifications of TiO_2 will have important consequences for hole and electron separation after photoexcitation. More details on this are presented in section 3.3. However, from the DOS analysis we can propose that in both cases PbO and PbO_2 modification of rutile will enhance the electron/hole separation. This arises since after excitation of PbO-TiO_2, the electron will be found in the surface and the hole on the nanocluster, while for PbO_2-TiO_2, the electron will be found on the PbO_2 nanocluster and the hole on the rutile surface, giving different mechanisms for electron-hole separation after photoexcitation.

This journal is © The Royal Society of Chemistry [year]

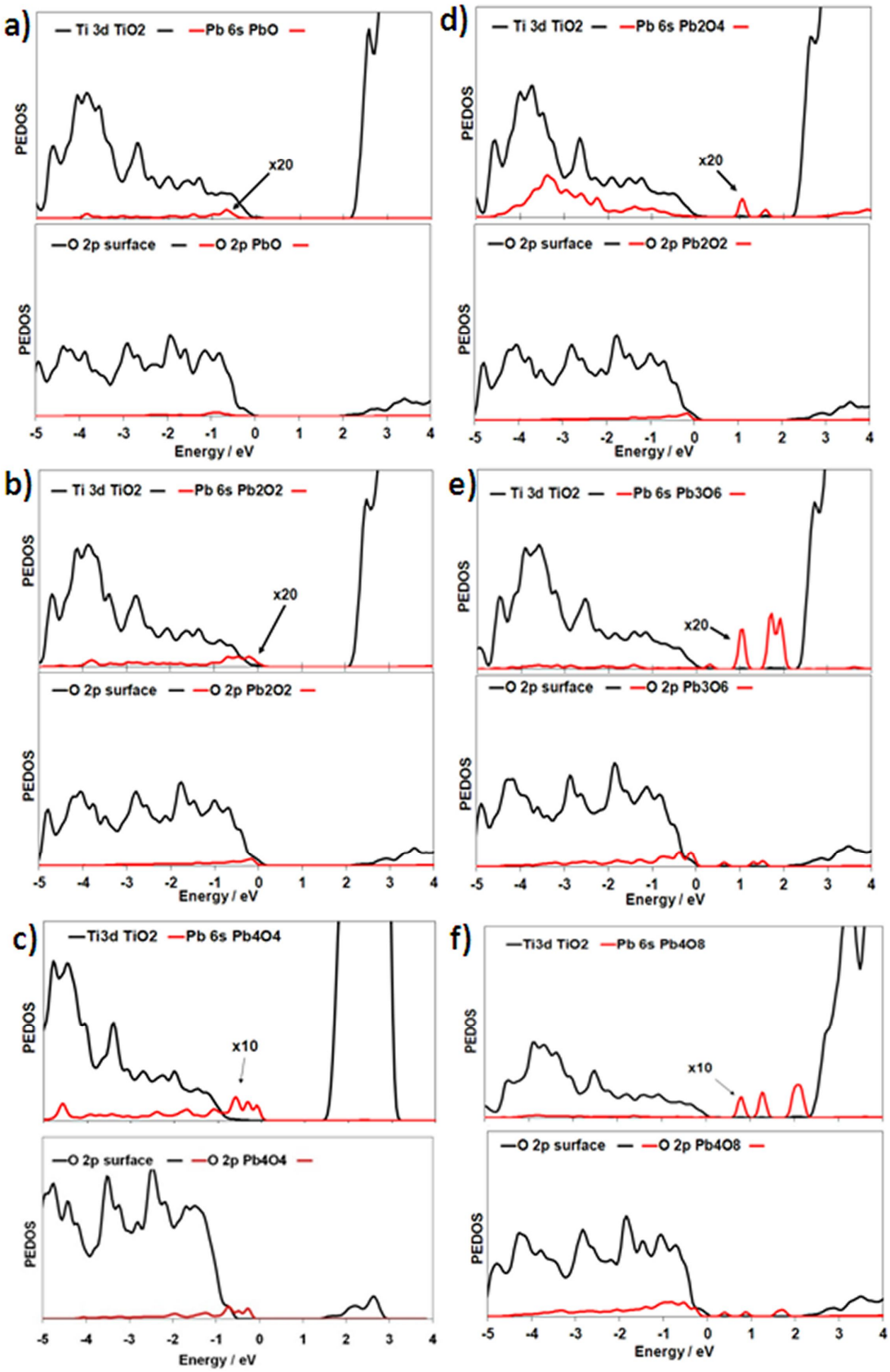


Fig. 2 Electronic density of states projected (PEDOS) onto Pb *6s,* O *2p* of the PbO and PbO_2 clusters and Ti 3*d,* and O *2p* states of the rutile (110) surface. In each set of plots, the energy zero is set to the top of the highest occupied electronic states, which is different for each PbO and PbO_2 modified TiO_2 system.

The Bader charges on Pb in PbO-TiO_2 nanoclusters are +1.20 electrons and in the PbO_2 nanoclusters, we computed Pb charges around +0.58 electrons. All Ti and O atomic charges are consistent with a Ti^{4+} and O^{2-} oxidation state.

Tin is another metal with two oxides, one of which has a stereochemically active lone pair. The present results for PbO and PbO_2 modified rutile can be compared to SnO and SnO_2[31,32] modified TiO_2 where our calculations show that the adsorption of SnO clusters on TiO_2 surfaces results in the introduction of the states above the valence band of TiO_2 which come from the Sn 5s – O 2p interaction and this shifts the valence band to higher energy, reducing the energy gap. In contrast, the adsorption of SnO_2 nanoclusters slightly affects the conduction band edge, with a small downwards shift of the CB edge observed in this case arising from empty Sn 5s states, in contrast to the position of the empty states in the energy gap from the PbO_2 nanoclusters.

3.2 PbO and PbO_2 nanoclusters supported on anatase (001)

Figure 3 presents the atomic structure of representative Pb_2O_2 and Pb_2O_4 nanoclusters supported on the TiO_2 anatase (001) surface. We investigate briefly if the different crystal structure of anatase compared to rutile can impact the properties after metal oxide cluster deposition. From these representative structures we conclude that the adsorption energies are similar to adsorption at the rutile (110) surface and the number of new bonds between clusters and surface are in the same range as well. The detailed metal-oxygen distances are presented in table 2 and the metal-oxygen distances are in the same range compared to PbO and PbO_2 modified rutile (110).

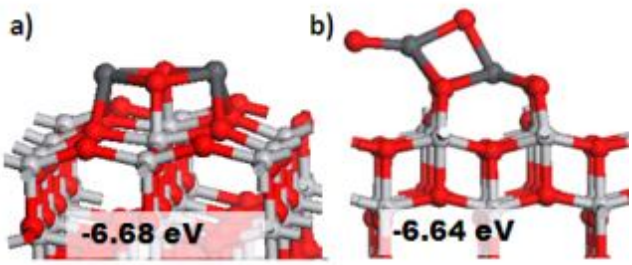


Fig. 3 Relaxed adsorption structures with adsorption energies given in eV for (a)Pb_2O_2, (b)Pb_2O_4clusters on TiO_2 anatase (001).

Table 2. New surface-cluster Pb-O bond distances for (PbO)n and (PbO_2)n clusters absorbed on TiO_2 anatase (001).

Distances / Å					
	Pb_c-O_s [a]	O_c-Ti_s [b]		Pb_c-O_s [a]	O_c-Ti [b]
Pb_2O_2	2.45; 2.45; 2.45; 2.44	1.92; 1.92	Pb_2O_4	2.11	1.90; 1.90; 1.86

[a] Pb from the cluster (**Pb_c**) and O from the surface (**O_s**) [b] O from the cluster (**O_c**) and Ti from the surface (**Ti_s**)

Figure 4 presents the PEDOS from the Pb 6*s* and O *2p* states of the nanocluster and the surface and Ti 3*d* and O *2p* states of anatase (001) after modification with PbO and PbO_2 nanoclusters. The PbO nanocluster introduces new states at the top of the valence band of anatase (001), while the PbO_2 nanocluster results in new states below the original conduction band of anatase (001). When comparing to the SnO_2 modification to rutile and anatase in refs. 31 and 32, where a notable crystal structure sensitivity was found in experiment and modelling, we can state that in contrast PbO_2 nanocluster modified TiO_2 shows no crystal structure sensitivity, with modifications to both rutile and anatase showing an effect on the energy gap. For SnO_2 nanocluster modified TiO_2, a positive effect on the visible light photocatalytic activity was only seen for rutile[31]. This difference arises for SnO_2 and PbO_2 modifications since the PbO_2 energy states lie lower in energy than the SnO_2 energy states and will create new electronic states in the original energy gaps of both TiO_2 polymorphs.

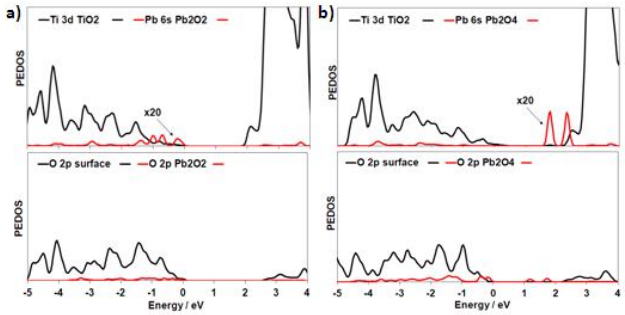


Fig. 4 The electronic density of states projected (PEDOS) onto Pb 6*s* and O *2p* states of the supported Pb_2O_2 and Pb_2O_4 clusters and the Ti3*d* and O *2p* states of the anatase (001) surface.

3.3. The Effect of Pb Oxidation state on the Excitation Energy and the Nature of the Photoexcited State.

The PEDOS plots of PbO and PbO_2 modified rutile (110) presented in figure 2 indicates two different VB and CB alignments, that are shown in the schematic diagram in figure 5.

For PbO supported nanoclusters the top of the valence band is from PbO nanocluster states and the surface Ti 3d states dominate the bottom of the conduction band of TiO_2. For PbO_2 supported nanoclusters the top of the valence band is from Ti 3d states while the PbO_2 states dominate the conduction band of TiO_2.

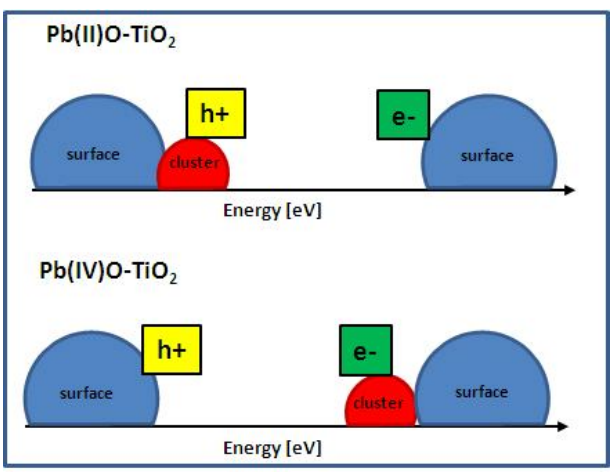


Fig. 5 Schematic diagram for indication of electron/hole localisation. h^+ and e^- indicate the electron and hole formed after photoexcitation.

These arrangements of the valence and conduction bands will enhance electron and hole separation upon photoexcitation, although the locations of hole and electrons will be different depending on oxidation state. From the schematic in figure 5, we propose that for PbO-modified TiO_2 photoexcitation will lead to the electron populating the conduction band which derives from rutile (110) surface, while the hole localization will be at the top of the PbO derived valence band. The localization of electron/hole for PbO_2-modified TiO_2 will be different: the electron will be found in conduction band states derived from empty Pb-O electronic states, while the hole should be localised on TiO_2 valence band derived states.

We examine charge separation by using the model of photoexcited state where a triplet electronic state is introduced. By construction this will have an electron in the conduction band and a hole located in the valence band. For rutile and anatase TiO_2, refs. 42, 43 and 45 have shown that this model produces a localised Ti^{3+} electronic state and a localised oxygen hole state (polarons), so long as DFT+U, with appropriate values of U on Ti and O, or hybrid DFT are used. These are necessary to localise the resulting polaronic states after photoexcitation. In the present systems, our intention is to study the location of the electron and hole after photoexcitation and demonstrate how changing the Pb oxidation state, which can be achieved by changing the Pb precursor in a synthesis, can lead to two different mechanisms of electron/hole separation.

Table 3 presents the vertical, relaxation and excitation energies for the bare rutile (110) surface and the Pb_4O_4-modified surface. For the Pb_2O_4-modified surface, we found that due to the close proximity of the empty Pb 6*s* states to the valence band, the photoexcited model with the strong DFT+U band gap underestimation gives an excitation energy that is close to 0 eV. Thus, we can highlight that while the simple photoexcited model has some merits, the underlying DFT functional plays an important role in its applicability. For PbO-modified TiO_2, we can compute these energies with more confidence.

Table 3: Excitation and relaxation energies for the triplet excited state in PbO- modified TiO_2 in eV. Also shown are the same energies for the bare rutile (110) surface.

Structure	E^{excite} / eV	E^{relax} / eV	$E^{vertical}$ / eV
Rutile TiO_2 (110)	1.69	0.52	2.21
Pb_4O_4 rutile 110	0.92	0.96	1.88

The energies for the bare rutile (110) surface have been discussed in ref. 45 and we point out here that the vertical energy is very similar to the valence-conduction band gap from the DOS and the excitation energy is lower as a result of relaxation following electron and hole formation.[42-45] Considering Pb_4O_4-modified rutile (110), the vertical and excitation energies are reduced by the surface modification, confirming the simple DOS analysis that PbO modification of TiO_2 will reduce the energy gap of TiO_2. The relaxation energy is also larger for PbO-modified rutile, which arises from the large gain in energy when the nanocluster strongly relaxes around the valence band hole, compared to relaxations in the (110) surface.

Figure 6 shows the spin density of the relaxed photoexcited state for the Pb_4O_4 and Pb_2O_4 nanoclusters supported on rutile (110). For Pb_4O_4-rutile (110) the electron is localised on a Ti site in the subsurface layer of rutile which assigned as a Ti^{3+} site. This can be confirmed by a Bader charge[47] of +1.66 electrons and spin magnetisation of +0.9 electrons. In contrast, the Ti^{4+} cation has a computed Bader Charge of +1.27 electrons and zero spin magnetisation. This localisation of electron gives an elongation of nearest Ti-O bonds of *ca.* 0.1 Å, which is typical for Ti-O bonds with a Ti^{3+} cation. The hole is localised on O from the PbO nanocluster with a computed Bader charge of +7.11 electrons and a computed spin magnetisation of +0.76 electrons.

In contrast to SnO-modified TiO_2,[32] where the hole is spread over an Sn-O bond, there is in the present structure little Pb contribution to the valence band hole. This would be consistent with the bulk findings that the lone pair effect diminishes as one goes down the group 14 column from Sn to Pb.[48]

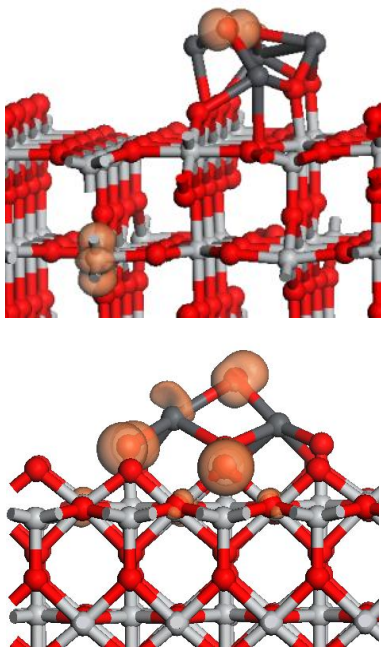


Fig. 6 Spin density and geometry of the photoexcited state in PbO and PbO_2-modified rutile (110)

Despite the issues with the very small energy gap and the computed singlet-triplet excitation energy, we briefly consider the nature of the photoexcited state for Pb_2O_4-modified rutile (110). With a Pb^{4+} oxidation state giving empty Pb states in the energy gap, the excited electron is distributed over a Pb atom from the cluster and two neighbouring oxygen atoms in the cluster. We characterise this Pb as a Pb^{3+} ion, confirmed by a Bader charge of +1.49 electrons (a Pb^{4+} cation has a computed Bader Charge of +0.58 electrons). The spin density in figure 6 shows that two oxygen atoms in the nanocluster also carry the electron, with Bader charges of +7.3 and +7.6 electrons for these O atoms and a computed spin magnetisation of +0.57 and +0.23 electrons, suggesting that the electron is spread over an O-Pb-O unit in the nanocluster. This gives an elongation of the cluster Pb-O bonds of *ca.* 0.3 Å. The valence band hole is localised on a bridging oxygen from the surface, with a computed Bader charge of +6.74 electrons and a spin magnetisation of +0.77 electrons, together

with an elongation of the nearest Ti-O bonds that involve this oxygen of 0.1 Å. The locations of the electron and hole in the Pb_2O_4-TiO_2 system appear to suggest that a less favourable separation of charge carriers is likely in this case, especially when compared with Pb_4O_4-modified TiO_2. This would have the consequence of more charge carrier recombination and lower photocatalytic activity.

3.3 Discussion

We have examined modifying TiO_2 rutile (110) and anatase (001) surfaces with PbO and PbO_2 nanoclusters to investigate: (1) the role of the metal oxidation state in the nanocluster in inducing visible light activation and charge recombination reduction, (2) the importance of the lone pair effect and (3) crystal sensitivity. Modification of rutile (110) and anatase (001) with PbO and PbO_2 nanoclusters is predicted to lead to a reduced energy gap compared to unmodified TiO_2. We expect that such structures will display visible light activity and, arising from the nature of the valence and conduction bands, a reduction in charge recombination after excitation. It is however, in the mechanism of band gap reduction and charge separation that we see differences between the two Pb oxidation states.

For PbO nanoclusters supported on rutile (110) and anatase (001) the results are consistent with previous theoretical and experimental findings for FeO_x,[28,29] NiO_x[30] and SnO_x[31,32] where the original TiO_2 band gap is reduced due to the introduction of electronic states from the nanoclusters above the TiO_2 valence band. The experimental studies using valence band X-ray photoelectron spectra confirm the reduction of band gap due to a rise of the valence band edge for FeO_x and NiO and are consistent with the modelling results, so that this mechanism of energy gap reduction should hold. A model of the photoexcited state confirms the reduction in the energy gap by modifying TiO_2 with SnO nanoclusters and highlights the charge separation upon photoexcitation.

However PbO_2 nanoclusters supported on rutile (110) and anatase (001), while leading to a predicted band gap reduction, present a striking difference in terms of the mechanism of band gap reduction and the nature of the valence and conduction band edges, somewhat similar to SnO_2[31] nanoclusters on rutile (110). In the latter, there is no rise in the TiO_2 valence band edge but the SnO_2 nanocluster states are present below the conduction band of TiO_2, giving a small reduction in the energy gap. For PbO_2-modified rutile, we find that the Pb-derived states lie well below the conduction band edge of TiO_2, which will reduce the energy gap. Unfortunately, the position of the states in the energy gap means that the simple photoexcited model does not work for computing excitation energies within the present computational set-up and in addition our results suggest that the spatial separation of electrons and holes will be less favourable in PbO_2-modified rutile compared to PbO-modified rutile.

Some support for this oxidation state effect comes from the recent experimental work on $ZnGa_2O_4$[33] which was modified with SnO and SnO_2 nanoclusters and the oxidation of Sn state was controlled by different precursors. In that work, only the modification with SnO resulted in a reduction of the band gap of $ZnGa_2O_4$. However, no atomic level explanation of this finding was given. However, the present results and those in refs. 31 and 32 along with these experimental hints do strongly indicate that the oxidation state of the metal in the nanocluster plays an important role in tuning the properties of photocatalyst.

In terms of the lone pair effect, for SnO-modified TiO_2, we find a strong effect on the energy gap with the valence band edge shifted upwards and derived from the Sn-6s-O2p interaction in the nanocluster. Analysis of the photoexcited state showed localisation of the hole on an Sn-O bond and the electron on a surface Ti atoms. For PbO, the shift of the TiO_2 band gap is due to the presence of Pb-6s-O-2p derived states from the PbO nanocluster pushing up the valence band edge. However the photoexcited states calculations suggests that the effect of the lone-pair is smaller compared to SnO-modified TiO_2[32], since the hole formed after photoexcitation is now also localised on oxygen in the nanocluster. Comparison with bulk indicates that the weakening of the lone pair effect is similar to bulk SnO and PbO.[48]

Another aspect of our analysis of the photoexcited of modified TiO_2 is new insights into the possibility of reducing electron-hole recombination and improving the photocatalytic properties. For PbO nanocluster modified rutile (110) and anatase (001) the hole is found on the nanocluster and the electron on a single Ti^{3+} in subsurface of the TiO_2 surface. In contrast, the PbO_2-TiO_2 photoexcited state shows electron-hole separation enhancement but with different locations of the hole and electron: the hole is localised on a bridging O atom from the surface while the electron is associated with an O-Pb-O structure in the PbO_2 nanocluster. Again the oxidation state of the metal in metal oxide supported nanoclusters presents an interesting approach to tuning of the photocatalytic properties of metal oxides.

Finally, comparing the properties of PbO and PbO_2-modified rutile (110) and anatase (001) for any crystal structure sensitivity previously found for SnO/SnO_2 modified anatase,[31] we have found that there is no sensitivity to crystal structure for lead oxide modified TiO_2.

Conclusions

We present DFT simulations of lead oxide nanoclusters supported on TiO_2 rutile (110) and anatase (001) surfaces. We found that the oxidation state of the metal in the supported metal oxide nanocluster plays an important role in defining the energy gap and the nature of the valence and conduction band edges. A reduction in the band gap of rutile and anatase TiO_2 can be achieved by modification with PbO or PbO_2 nanoclusters. Different Pb oxidation states show different electron/hole localisation upon photoexcitation and hence different mechanisms for charge separation. The enhancement in electron/hole separation will improve photocatalytic properties over pure TiO_2. Photoexcited calculations for PbO nanoclusters supported on rutile (110) show the decreasing effect of the lone-pair which is similar to bulk. There is no crystal sensitivity reported for adsorbed PbO and PbO_2 nanoclusters on rutile (110) and anatase (001). Finally the current set-up of VB-CB shows reduction in the band gap comparing to TiO_2 origin and The present results give interesting insights into the possibility in tuning the photocatalytic properties by metal oxidation state, lone pair effect and crystal structure for developing new photocatalysts.

This journal is © The Royal Society of Chemistry [year]

Acknowledgements

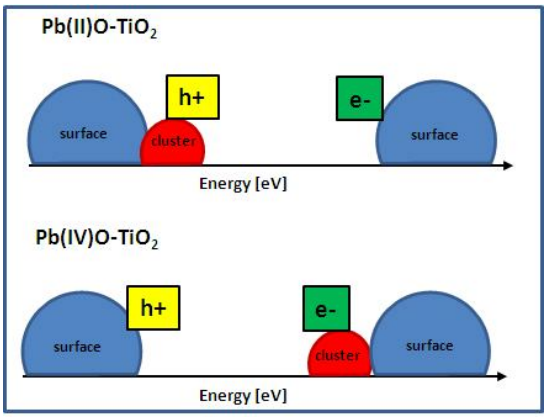
We acknowledge support from Science Foundation Ireland (SFI) through the Starting Investigator Research Grant Program, project "EMOIN" grant number SFI 09/SIRG/I1620. Access to computing resources at Tyndall is funded by SFI, by the SFI and Higher Education Authority funded Irish Centre for High End Computing and by the European Union FP7 Research Infrastructures Program PRACE, through the DECI-8 program, contracts RI-261557 and RI-283493. We acknowledge support from the European Union through the COST Action CM1104 "Reducible Oxide Chemistry, Structure and Functions".

Notes and references

Tyndall National Institute, University College Cork, Lee Maltings, Dyke Parade, Cork; Ireland. E-mail: michael.nolan@tyndall.ie

1. A. Fujishima, X. Zhang, and D. A. Tryk, *Surf. Sci. Rep.,* 2008, **63**, 515
2. M. Ni, M. K. H. Leung, D. Y. C. Leung and K. Sumathy, *Renew. Sust. Energ. Rev.,* 2007, **11**, 401
3. J. Zhao, C. Chen and W. Ma, *Top. Catal.,* 2005, **35**, 269
4. H. Choi, M. G. Antoniou, M. Pelaez, A. Delacruz, J. Shoemaker and D. D. Dionysiou, *Environ. Sci. Technol.,* 2007, **41**, 7530
5. H. Yu, H. Irie, Y. Shimodaira, Y. Hosogi, Y. Kuroda, M. Miyauchi, and K. Hashimoto, *J. Phys. Chem. C*, 2010, **114**, 16481
6. A. Kubacka, M. Fernandez-Garcia and G. Colon, *Chem. Rev.,* 2012, **112**, 1555
7. J. G. Yu, Q. J. Xiang, M. H. Zhou and X. Y. Zhou, *Appl Cat. B Environ.,* 2009, **90**, 595
8. H. W. Peng, J. B. Li, S. S. Li and J. B. Xia, *J. Phys. Condens. Matter*, 2008, **20**, 125207
9. C. Di Valentin, E. Finazzi, G. Pacchioni, A. Selloni, S. Livarghi, M. C. Paganini and E. Giamello, *Chem. Phys.,* 2007, **339**, 44
10. A. Iwaszuk and M. Nolan, *J. Phys. Chem. C,* 2011, **115**, 12995
11. X. L. Nie, S. P. Zhou, G. Maeng, and K. Sohlberg, K. *Int. J. Photoenergy,* 2009, article 294042
12. C. Di Valentin, G. Pacchioni, H. Onishi and A. Kudo, *Chem. Phys. Lett.,* 2009, **469**, 166
13. R. Long and N. J. English, *J. Phys. Chem. C*, 2010, **114**, 11984
14. W. Zheng, A. Bhattcahrayya, P. Wu, Z. Chen, J. Highfield, Z. L. Dong, and R. Xu, *J. Phys. Chem. C,* 2010, **114**, 7063
15. Y. Q. Gai, J. B. Li, S. S. Li, J. B. Xia and S. H. Wei, *Phys. Rev. Lett.,* 2009, **102**, 036402
16. W. G. Zhu, X. F. Qiu, V. Iancu, X. Q. Chen, H. Pan, W. Wang, N. M. Dimitrijevic, T. Rajh, H. M. Meyer, M. P. Paranthaman, G. Stocks, H. H. Weitering, B. H. Gu, G. Eres and Z. Y. Zhang, *Phys. Rev. Lett.,* 2009, **103**, 2264101
17. J. Zhang, C. X. Pan, P. F. Fang, J. H. Wie and R. Xiong, *ACS Appl. Mater. Interfaces,* 2010, **2**, 1173
18. Q. Jin, M. Fujishima and H. Tada, *J. Phys. Chem C,* 2011, **115**, 6478
19. R. Long and N. J. English, *Appl. Phys. Lett.,* 2009, **94**, 132102
20. N. Murakami, T. Chiyoya, T. Tsubota and T. Ohno, *Appl. Catal. A,* 2008, **348**, 148.
21. H. Wang and J. P. Lewis, *Journal of Physics: Condensed Matter,* 2006**, 18**, 421
22. H. Yu, H. Irie, Y. Shimodaira, Y. Hosogi, Y. Kuroda, M. Miyauchi, K. Hashimoto, *J. Phys. Chem. C,* 2010, **114**, 16481
23. M. Fujishima, Q. Jin, H. Yamamoto, H. Tada and M. Nolan, *Phys. Chem. Chem. Phys.,* 2012, **14**, 705
24. J. A. Libera, J. W. Elam, N. F. Sather, T. M. Rajh and N. M. Dimitrijevic, *Chem. Mater.,* 2010, **22**, 409
25. L. Kong, Z. Jiang, T. Xiao, L. Lu, M.O. Jones and P. P. Edwards, *Chem. Commun.,* 2011, **47**, 5512.
26. H. Cheng, B. Huang, Y. Dai, X. Qin and X. Zhang, *Langmuir,* 2010, **26**, 6618
27. S. J. Hong, S. Lee, J .S. Jang and J. S. Lee, *Energy Environ. Sci.,* 2011, **4**, 1781
28. H. Tada, Q. Jin, H. Nishijima, H. Yamamoto, M. Fujishima, S. Okuoka, T. Hattori, Y. Sumida and H. Kobayashi, *Angew Chem.,* 2011, **50**, 3501
29. M. Nolan, *Phys. Chem. Chem. Phys.,* 2011, **13**, 18194
30. A. Iwaszuk, M. Nolan, Q. Jin, M. Fujishima and H. Tada, *J. Phys. Chem C*, 2013, **117**, 2709
31. Q. Jin, M. Fujishima, M. Nolan, A. Iwaszuk and H. Tada, *J. Phys. Chem. C,* 2012, **116**, 12621
32. A. Iwaszuk and M. Nolan, *J. Mat. Chem. A,* 2013, doi:10.1039/C3TA10647K
33. V. B. R. Boppana and R. F. Lobo, *ACS Catal.* 2011, **1**, 923.
34. G. Kresse and J. Hafner, *Phys Rev. B: Condens. Matter,* 1994, **49**, 1425
35. P. E. Blöchl, *Phys. Rev. B* 1994, **50**, 17953
36. J. P. Perdew, J. A. Chevary, S. H. Vosko, K. A. Jackson, M. R. Pederson, D. J. Singh and C. Fiolhais, *Phys Rev. B: Condens. Matter,* 1993, **46**, 6671.
37. B. J. Morgan and G. W. Watson, *Surf. Sci.,* 2007, **601**, 5034
38. V. I. Anisimov, J. Zaanen and O. K. Andersen, *Phys Rev. B: Condens. Matter,* 1991, **44**, 943.
39. S. L. Dudarev, G. A. Botton, S. Y. Savrasov, C. J. Humphreys and A. P. Sutton, *Phys Rev. B: Condens. Matter,* 1998, **57**, 1505
40. M. V. Ganduglia-Pirovano, A. Hofmann and J. Sauer, *Surf. Sci. Rep.,* 2007, **62**, 219.
41. M. Nolan, S. Grigoleit, D. C Sayle, S. C Parker and G. W. Watson, *Surf. Sci.,* 2005, **576**, 217.
42. C. Di Valentin and A. Selloni, *J. Phys. Chem. Lett.* 2011, **2,** 222
43. A. Jedidi, A. Markovits, C. Minot, S. Bouzriba and A. Abderraba, *Langmuir,* 2010, **26**, 16232
44. D. Munoz Ramos, P. V. Sushko and A. L. Shluger, *Phys Rev. B: Condens. Matter,* 2012, **85**, 024120
45. M. Nolan, *ACS Appl. Mater. Interfaces,* 2012, **4**, 5386
46. A. Walsh and G. W. Watson, *Journal of Solid State Chemistry,* 2005, **178**, 1422
47. G. Henkelman, A. Arnaldsson and H. Jónsson, *Comput. Mater. Sci.,* 2006, **36**, 25
48. A. Walsh, D. J. Payne, R. G. Egdell and G. W. Watson, *Chemical Society Reviews* 2001, **40**, 4455

Graphic Abstract



The photocatalytic properties of lead oxide modified TiO_2 are controlled by the oxidation state of lead.

This journal is © The Royal Society of Chemistry [year]